Received: 5 June 2021 | Revised: 26 October 2021 | Accepted: 1 November 2021

DOI: 10.1111/1750-3841.15996



Journal of Food Science WILEY

# A single-walled carbon nanotubes-based electrochemical impedance immunosensor for on-site detection of *Listeria monocytogenes*

**Bog Eum Lee**[1] | **Taiyoung Kang**[2] | **Daniel Jenkins**[2] | **Yong Li**[1] | **Marisa M. Wall**[3] | **Soojin Jun**[1]

[1] Department of Human Nutrition, Food, and Animal Sciences, University of Hawaii, Honolulu, Hawaii, USA

[2] Department of Molecular Biosciences and Bioengineering, University of Hawaii, Honolulu, Hawaii, USA

[3] USDA-ARS Daniel K. Inouye U.S. Pacific Basin Agricultural Research Center, Hilo, Hawaii, USA

**Correspondence**
Soojin Jun, Department of Human Nutrition, Food, and Animal Sciences, University of Hawaii, Honolulu, Hawaii 96822, USA.
Email: soojin@hawaii.edu

**Abstract:** Real-time and sensitive detection of pathogenic bacteria in food is in high demand to ensure food safety. In this study, a single-walled carbon nanotubes (SWCNTs)-based electrochemical impedance immunosensor for on-site detection of *Listeria monocytogenes* (*L. monocytogenes*) was developed. A gold-plated wire was functionalized using polyethylenimine (PEI), SWCNTs, streptavidin, biotinylated *L. monocytogenes* antibodies, and bovine serum albumin (BSA). A linear relationship ($R^2 = 0.982$) between the electron transfer resistance measurements and concentrations of *L. monocytogenes* within the range of $10^3$–$10^8$ CFU/ml was observed. In addition, the sensor demonstrated high selectivity towards the target in the presence of other bacterial cells such as *Salmonella* Typhimurium *and Escherichia coli* O157:H7. To facilitate the demand for on-site detection, the sensor was integrated into a smartphone-controlled biosensor platform, consisting of a compact potentiostat device and a smartphone. The signals from the proposed platform were compared with a conventional potentiostat using the immunosensor interacted with *L. monocytogenes* ($10^3$–$10^5$ CFU/ml). The signals obtained with both instruments showed high consistency. Recovery percentages of lettuce homogenate spiked with $10^3$, $10^4$, and $10^5$ CFU/ml of *L. monocytogenes* obtained with the portable platform were 90.21, 90.44, and 93.69, respectively. The presented on-site applicable SWCNT-based immunosensor platform was shown to have a high potential to be used in field settings for food and agricultural applications.

**KEYWORDS**
biosensor, EIS, food pathogens, portable, SWCNT

**Practical Application:** The developed immunosensor was developed for on-site detection of *L. monocytogenes*. The limit of detection of the sensor was $10^3$ CFU/ml with a detection time of 10 min. In order to facilitate the requirements for effective on-site screening for food safety, the sensor was integrated into a smartphone-controlled platform, so that the bio-molecular interactions were converted into impedance signals and transmitted wirelessly to a smartphone by a hand-held EIS transducer.

  

## 1 | INTRODUCTION

Food safety has attracted significant attention due to continued outbreaks. It was estimated that in the United States, 1 in 6 people are sickened from consumption of contaminated foods each year and 3,000 die (CDC, 2018). *Listeria monocytogenes* is one of the most dangerous foodborne pathogens which causes a fatal disease, listeriosis. *L. monocytogenes* is widely distributed in the environment, and there has been an increasing trend in fresh produce-associated listeriosis outbreaks, such as chopped celery, whole cantaloupes, lettuces, and packaged salads (Zhu et al., 2017).

Conventional methods for detection and identification of pathogenic microorganisms include traditional culture plating (gold standard method), polymerase chain reaction (PCR), and enzyme-linked immune-sorbent assay (ELISA; Chen et al., 2016; Jadhav et al., 2012; Sharma & Mutharasan, 2013). Although the above methods are highly reliable, they are time-consuming and labor-intensive. In addition, these analyses require operations by well-trained personnel in laboratory settings. As a consequence, there is a real need for the development of sensitive, accurate, and rapid methods that can be employed for on-site detection (Arora et al., 2011; Majumdar et al., 2013).

Biosensor-based detection method has been proposed as a promising alternative due to its simplicity, cost-efficiency, and potential field applications (Mello & Kubota, 2002). In particular, electrochemical impedance spectroscopy (EIS)-based biosensor has received much attention as it allows for a label-free detection of various analytes with high sensitivity (Bogomolova et al., 2009). The EIS-based immunosensor analyzes changes in the electron transfer resistance ($R_{et}$) at a bio-interface, which arises from the antigen-antibody interaction. The $R_{et}$ is obtained by measuring the response of an electrochemical cell to a small amplitude of sinusoidal voltage as a function of wide range of frequency (Prodromidis 2010; Wang et al., 2012). The forte of this technique is its ability to measure subtle changes in the electrical properties of an electrode surface, thus elevating the sensitivity (Chowdhury et al., 2012; Lu et al., 2013).

Numerous nanomaterials-based biosensors have been developed for improved sensitivity and response time (Ferrier et al., 2015; Rodriguez et al., 2015). Among a large variety of nanomaterials, single-walled carbon nanotube (SWCNT) has been suggested as the most applicable nanomaterial due to its unique properties. SWCNT offers significant advantages such as fast electron transfer capability, high surface area, and physicochemical stability (Allen et al., 2007; Heller et al., 2008).

In this study, a SWCNTs-based immunosensor was developed and integrated into a smartphone-controlled EIS platform for the detection of *L. monocytogenes*. In this platform, the bio-molecular interactions were converted into impedance signals and transmitted wirelessly to a smartphone by a hand-held EIS transducer. An Android application was developed to control the electrochemical measuring process, and the results of analysis are displayed graphically in real-time. The analytical performance of the proposed smartphone-controlled biosensor was compared with a reference laboratory potentiostat.

## 2 | MATERIALS AND METHODS

### 2.1 | Microwire sensor fabrication

The microwire functionalization method was adapted from Yamada et al. (2014) with minor modifications. 7% gold-plated tungsten wires (diameter: 50 μm) purchased from ESPI Metals (Ashland, OR, USA) were cut into 25 mm length, sonicated in distilled water, and cleansed with 70% alcohol for 5 min. The wires were then dried in a furnace at 175°C for 10 min. The sanitized microwires were mounted onto a programmable XYZ stage (Franklin Mechanical & Control Inc., Gilroy, CA, USA) and the COSMOS operating program for the surface modifications (Velmex, Inc., Bloomfield, NY, USA). For the microwire surface functionalization, 1% polyethylenimine (PEI, branched, average MW ~25,000, product no. 40827) and 0.01% SWCNTs (SWNT PD1.5L; NanoLab, Inc., Waltham, MA, USA) were dispersed in N,N-dimethylformamide (DMF; Sigma Aldrich, St. Louis, MO, USA) sequentially by dipping and withdrawing motions at a velocity of 6 mm/min. Thereafter, 5 μl of streptavidin (#85878, Sigma Aldrich), 5 μl of biotinylated polyclonal *L. monocytogenes* antibodies (#PA 1–85650; Thermo Fisher Scientific, Waltham, MA, USA), and 5% bovine serum albumin (BSA; #A3294, Sigma Aldrich) were dropped on the PEI-SWCNTs coated wires in a stepwise manner for the recognition of antigen using polydimethylsiloxane (PDMS; #1024001; Dow Corning, Midland, MI, USA) as a support.

### 2.2 | Microbial preparation

Frozen stock cultures of *Escherichia coli* O157:H7, *L. monocytogenes* (F2365), and *Salmonella* Typhimurium (ATCC 14028) were obtained from the Food Microbiology Lab, University of Hawaii. All experiments were conducted in this lab, a certified biosafety level II laboratory. 100 μl of each bacterial strain was cultured separately in 10 ml of tryptic soy broth (BBL™ Trypticase ™ soy broth; BD Diagnostic Systems, Franklin Lakes, NJ, USA) and incubated for 24 h at 37°C. The serial dilution was performed using

**TABLE 1** Cell concentrations of each bacterium measured in pure and microbial cocktail solutions for specificity and selectivity test

| Bacteria | Concentrations (CFU/ml) | |
|---|---|---|
| *L. monocytogenes*[a] | $1.97 \times 10^4$ | |
| *E. coli* O157:H7 | $2.63 \times 10^4$ | |
| *S.* Typhimurium | $1.55 \times 10^4$ | |
| | Concentrations (CFU/ml) | |
| Bacterial mixture | Target | Nontarget |
| *L. monocytogenes*[a] + *E. coli O157:H7* | $2.62 \times 10^4$ | $1.73 \times 10^4$ |
| *L. monocytogenes*[a] + *S.* Typhimurium | $1.92 \times 10^4$ | $1.83 \times 10^4$ |

[a]Target.

0.1% peptone water to achieve a range of desired concentrations of each culture. Microbial cocktail samples were prepared by transferring 100 µl of *L. monocytogenes* culture to 900 µl of nontarget bacteria suspension. The initial concentrations of *E. coli* O157:H7, *S.* Typhimurium, *L. monocytogenes* were obtained by the plate counting method on OXOID MacConkey agar (Thermo Fisher Scientific, Waltham, MA, USA), Xylose Lysine Desoxycholate agar (BBL™ XLD Agar Prepared Media Stacker ™ Plates; BD diagnostic systems), and PALCAM *Listeria* selective agar (Difco™ PALCAM Medium Base) with antimicrobic supplement, respectively. The concentrations of the individual bacterial species in pure and microbial cocktail samples are summarized in Table 1.

## 2.3 | The smartphone-controlled biosensor system

The smartphone-controlled biosensor module designed and validated in our previous work (Jenkins et al., 2019) is comprised of three parts: a functionalized microwire sensor, a compact ABE-Stat potentiostat operated with a smartphone app (Figure 1a). The potentiostat device is fully wireless-enabled by integrating Bluetooth and Wi-fi modules. The commands for EIS analysis originated from an Android app that interfaced the smartphone with the potentiostat. A detailed abridged schematic of ABE-Stat analog networks can be found in the study from Jenkins et al. (2019). A reference laboratory potentiostat (µ-Autolab type III potentiostatic frequency response analyzer (FRA) equipped with NOVA software version 1.6, Metrohm Autolab USA Inc., Riverview, FL, USA) was used to compare the performance of the smartphone-controlled potentiostat. The EIS analysis was performed with both systems under the same conditions and parameters described below.

## 2.4 | Detection of *L. monocytogenes*

A 9-well plate (Figure 1b) was designed using a SolidWorks software (Dassaults System Solidworks Corp., Waltham, MA, USA) and was 3D-printed using a photopolymer resin (Form 2; Formlabs, Somerville, MA, USA). In order to enhance the recognition of the target, the designed 9-well plate was equipped with a vibration motor (Gear Motor, Uxcell, Hong Kong). 500 µl of the bacterial sample was placed in each well, and the functionalized microwire was placed to the well for 5 min, allowing for antibody-antigen interaction. Applying slight agitation aided in enhancing the sensitivity of the sensor by 1 − log for the detection of *E. coli* K12 (data not shown). Therefore, constant agitation was applied to the plate to enhance the bioaffinity reaction. Sensitivity testing was conducted to determine the limit of detection (LOD) of the functionalized microwire. Serial dilutions of *L. monocytogenes* were prepared from the activated culture and tested with the microwire. The specificity of the fabricated biosensor towards the target was evaluated by also testing with pure cultures of *S.* Typhimurium and *E. coli* O157:H7 at a concentration of approximately $10^4$ CFU/ml alone, and in mixed solutions with *L. monocytogenes*. A total of the sensing time including cell concentration and signal measurement was approximately 10 min.

## 2.5 | Preparation of lettuce homogenate

Lettuce was purchased from a local grocery store in Honolulu, Hawaii. 10 g of lettuce mixed with 90 ml of sterilized PBS was homogenized using a stomacher (400 Circulator; Seward Inc., Bohemia, NY, USA) at 260 rpm for 10 min (Mao et al., 2016). The lettuce homogenate was spiked with *L. monocytogenes* to achieve final concentrations ranging from $10^3$ to $10^5$ CFU/ml. The number of viable cells was plate counted on the PALCAM *Listeria* selective agar.

## 2.6 | Impedance measurement

The electrochemical cell was constructed with a conventional three-electrode configuration in an electrolyte solution. The electrolyte solution was prepared by dissolving 5 mM $K_3Fe(CN)_6$ (#244023), 5 mM $K_4Fe(CN)_6$ (#P3289), and 0.1 M KCl (#P9541) in distilled water (#6442; Sigma-Aldrich). The functionalized microwire was used as a working electrode (WE), a platinum electrode (product no. CHI 115, ∅ = 0.5 mm; CH Instruments, Inc., Austin, TX, USA) was used as a counter electrode, and a saturated Ag/AgCl electrode (catalog no. A57194; VWR International, Brisbane, CA, USA) served as a reference

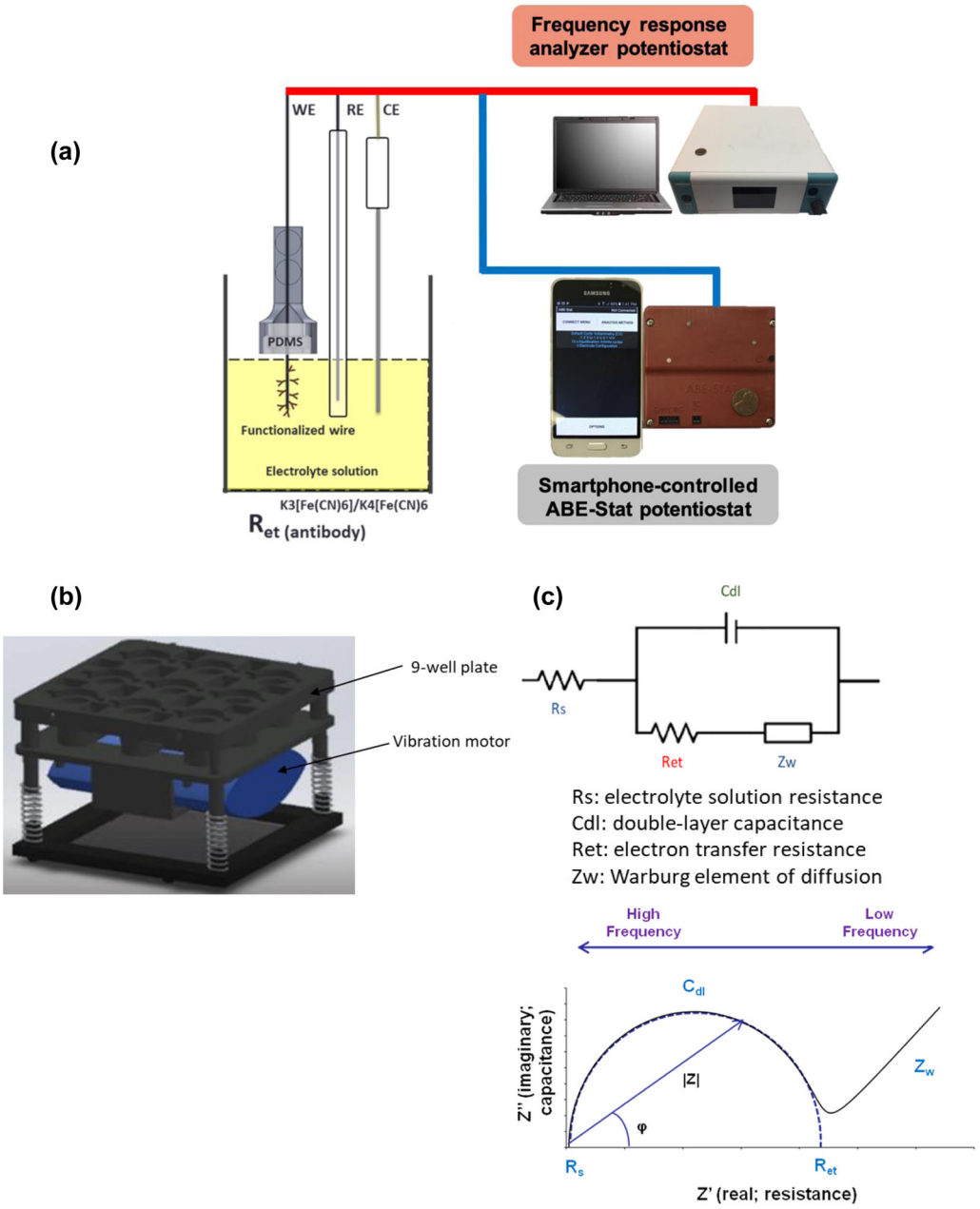


**FIGURE 1** (a) Schematics of reference laboratory potentiostat and smartphone-controlled biosensor platform, (b) 9-well plate equipped with a vibration motor for the enhanced recognition, and (c) Randles equivalent circuit of faradaic EIS measurement and the Nyquist plot ($Z'$ vs. $Z''$)

electrode. We measured the electrochemical impedance over the scanning frequency between 0.1 Hz and 100 kHz at a DC bias potential of 200 mV, and a peak AC 10 mV. The experimental data were represented by the Nyquist plots, which were obtained from the reference laboratory device were analyzed using the NOVA software. The value of $R_{et}$ was estimated from the Randles equivalent circuit model as shown in Figure 1c. The Nyquist plots from ABE-Stat were analyzed by Matlab software (Mathworks, Natick, MA, USA) using the same equivalent circuit model. The changes of electron transfer resistance ($\Delta R_{et}$) at the sensor interface due to the attachment of bacterial cells at the electrode–film interface were calculated using the equation given by:

$$\Delta R_{et} = R_{et}\,(\text{antibody} - \text{bacteria}) - R_{et}\,(\text{antibody}) \quad (1)$$

## 2.7 | Data analysis

Three replications were performed for each experiment. The electrochemical impedance signals were averaged,

and standard deviations were expressed as error bars in the graphs. One way analysis of variance (ANOVA) was carried out between the mean values, followed by Duncan's multiple range tests at the confidence level of 95% using a statistical analysis software (SPSS Inc., Chicago, IL, USA). The statistical analysis of the average of the electrochemical impedance measured by the portable and reference devices were conducted using a paired *t* test 95% confidence level.

## 3 | RESULTS AND DISCUSSION

### 3.1 | Monitoring the surface functionalization of the anti-*L. monocytogenes* immunosensor

EIS data are commonly displayed using a Nyquist plot, consisting of the imaginary impedance component ($Z$") against the real impedance component ($Z$') as shown in Figure 1c. A typical shape of a Nyquist plot includes a semicircle region lying on the real axis followed by a straight line. The semicircle part falls in the high frequency range is dominated by electron transfer process, while the tail part falls in the low frequency range is dominated by diffusion process (Yang & Bashir, 2008). At a high frequency (100 kHz), the impedance arises from the electrolyte solution itself, whereas at a lower frequency (0.1 Hz), the impedance results from the resistance to the flow of electrons to the electrode surface. The Nyquist plot was translated into an equivalent circuit model, Randles circuit, to investigate the electrical parameters including the electron transfer resistance ($R_{et}$). When the imaginary impedance is zero, the intercept of the semicircle with the $x$-axis indicates electrolyte solution resistance ($R_s$). The diameter of the semicircle is estimated to be the electron transfer resistance ($R_{et}$) of the working electrode.

The stepwise surface modification step was characterized by the EIS measurements in the presence of the redox couple $[Fe(CN)_6^{4-/3-}]$ (Figure 2a). The SWCNTs adsorbed onto the surface of Au/PEI layer due to the amine–nanotube interaction. Amine groups of PEI have a high-binding affinity for SWCNTs, forming polymer-SWCNT films (Rouse et al., 2004). The PEI-SWCNTs modified surface is able to bind with the negatively charged streptavidin via electrostatic and hydrophobic interactions (Lu et al., 2013; Yamada et al., 2014). Streptavidin on the modified surface links with the biotinylated antibodies with the well-known streptavidin–biotin interaction (Darst et al., 1991).

The average $R_{et}$ of a bare microwire was 0.317 ± 0.005 kΩ. When the bare microwire was coated with PEI, the $R_{et}$ increased to 2.99 kΩ, followed by a significant decrease to 0.68 kΩ when SWCNTs were introduced to the surface. The dramatic decrease in the $R_{et}$ demonstrated that the SWCNT layer enhanced the conductivity through electrode/electrolyte interface. Further adsorption of streptavidin, antibody, and BSA on the Au/PEI/SWCNT modified microwire increased the $R_{et}$ to 1.85, 2.97, and 3.21 kΩ, respectively. On the electrode, the electron transfer between the redox probe, $[Fe(CN)_6]^{4-/3-}$ and the electrode occurs by tunneling of electrons through the coating layers or through the unblocked sites on the surface. Hence, the surface passivation influences the $R_{et}$ at the electrode/electrolyte solution interface.

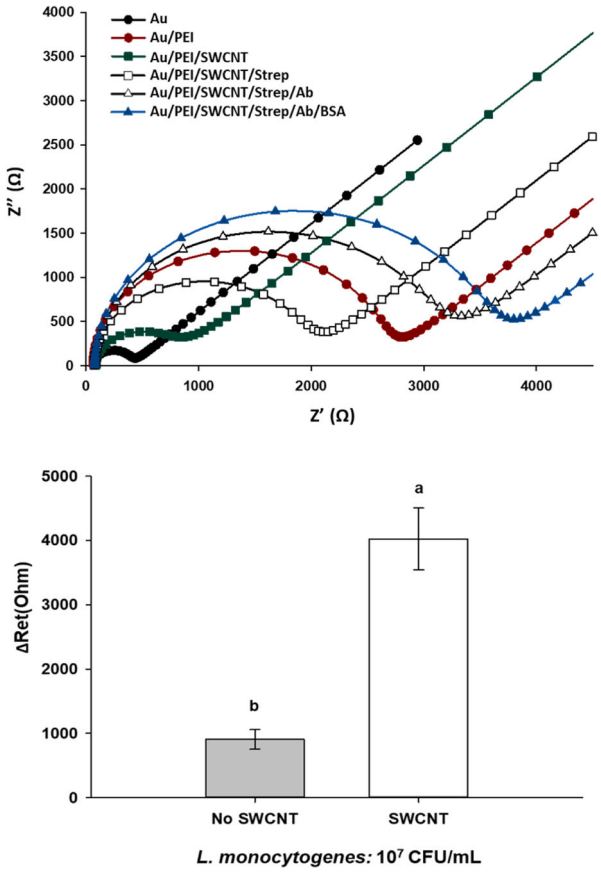


**FIGURE 2** Impedance spectra of the electrode corresponding to stepwise modifications (a) and change in the electron transfer resistance in response to *L. monocytogenes* captured on the sensor with and without SWCNTs (b)

The observed increase in $R_{et}$ implies that the microwire is successfully functionalized and the surface coatings hinder the charge transfer of the $[Fe(CN)_6^{4-/3-}]$ redox couple to the surface of the electrode (Liu et al., 2011). These trends are consistent with other studies as well (Bourigua et al., 2010; Chen et al., 2012). The effect of SWCNTs on the signal enhancement was evaluated as well. Figure 2b demonstrates that $\Delta R_{et}$ of 4.02 kΩ was observed when the SWCNTs integrated sensor was exposed to $10^7$ CFU/ml *L. monocytogenes* solution. However, $\Delta R_{et}$ of 0.90 kΩ was

measured with the sensor without SWCNTs when interacted with the same *L. monocytogenes* concentration. The increase in $\Delta R_{et}$ may be attributed to the elevated surface area due to SWCNTs, which serves as an active binding platform of the antibodies.

## 3.2 | Performance of the *L. monocytogenes* biosensor

The sensors were exposed to stepwise increasing concentrations of *L. monocytogenes* and microbial cocktail solutions to assess the performance of the sensor (sensitivity, selectivity, and specificity) before deployed in a real food sample. These were evaluated with the conventional laboratory instrument. The sensitivity of the sensor was evaluated with serially diluted *L. monocytogenes* cultures. A linear relationship was obtained in the range of $10^3$ to $10^8$ CFU/ml with a LOD of $1.4 \times 10^3$ CFU/ml (correlation coefficient $R^2 = 0.982$; Figure 3a). Each data point represented a mean value obtained from three independent microwire sensors; error bars represented the standard deviation of the three measurements. As expected, a greater $\Delta R_{et}$ was measured as the bacterial concentrations in the samples increased, that is, increased electron transfer resistance of a redox probe of $Fe(CN)_6^{3-/4-}$ at the interface between electrode and electrolyte. This change in the electrical properties of the sensor could be attributed to the highly insulating properties of the cell membrane. It was found that the conductivity of the cell membrane is significantly lower (approximately $10^{-7}$ S/m) than the interior of a cell (1 S/m; Jain et al., 2012). As a result, the attachment of the bacterial cells retards the interfacial electron–transfer kinetics and thus increases the $R_{et}$.

Specificity is a crucial factor in developing a microorganism detection tool. The specificity of the anti-*L. monocytogenes* sensor was evaluated by comparing the signals against pure *L. monocytogenes* culture ($10^4$ CFU/ml) to pure *E. coli* O157:H7 and *S.* Typhimurium ($10^4$ CFU/ml), individually. Data represented in Figure 3b indicate that the sensor's response to pure culture of *E. coli* O157:H7 and *S.* Typhimurium resulted in $\Delta R_{et}$ values of 220 and 185 Ω, respectively. This may be partly due to the nonspecific binding at the surface of the electrode. However, when the sensor was exposed to pure suspension of *L. monocytogenes* ($10^4$ CFU/ml), a significant increase in the $\Delta R_{et}$ was observed. This recognition is achieved by the induced immune complex reaction on the surface of the sensor. These results indicate that the anti-*L. monocytogenes* sensor exhibits negligible responses to the nontargets, demonstrating high specificity to the target over the other bacteria.

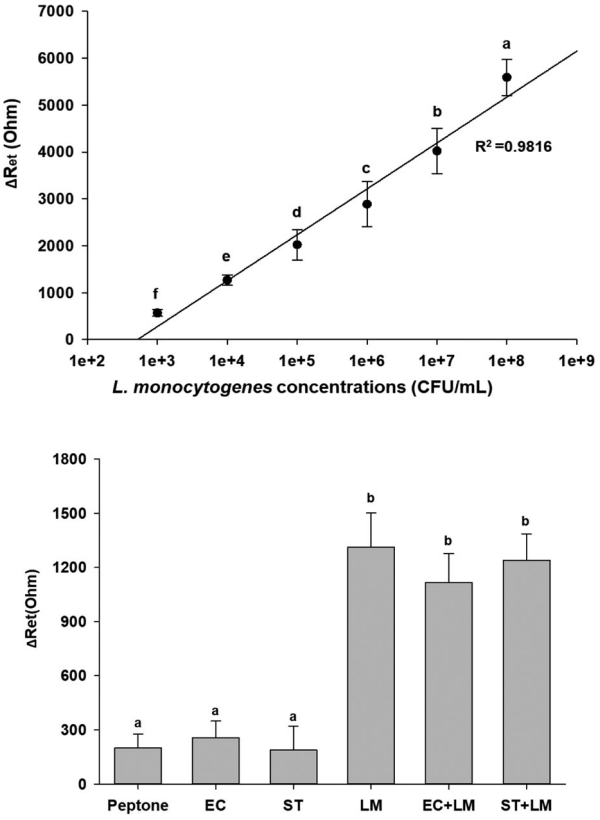


**FIGURE 3** Relationship between changes in the electron transfer resistance and concentrations of *L. monocytogenes* ($10^3$–$10^8$ CFU/ml) bound to the sensor (a) and its specificity and selectivity testing for *L. monocytogenes*. Acronyms represent pure bacteria suspension and bacterial mixtures; EC (*E. coli O157:H7*), ST (*S. Typhimurium*), LM (*L. monocytogenes*), EC + LM (a mix of *E. coli O157:H7* and *L. monocytogenes*), and ST + LM (a mix of *S. Typhimurium* and *L. monocytogenes*) (b)

The selectivity of the biosensor was studied to evaluate the possible interference on the sensing signals. The selectivity of the proposed sensor towards *L. monocytogenes* was evaluated by challenging it with microbial mixture samples (*L. monocytogenes* and *E. coli* O157:H7, and *L. monocytogenes* and *S.* Typhimurium at $10^4$ CFU/ml concentrations). When the sensor interacted with mixtures of EC + LM and ST + LM, the obtained $\Delta R_{et}$ values were 1,025 ± 35 and 1,260 ± 198 Ω, respectively. These signals were close to the sensor's response when it was introduced to $10^4$ CFU/ml of pure *L. monocytogenes*, 1,205 ± 350 Ω. These results demonstrate that the electron transfer behavior remained unchanged with the existence of nontarget bacteria, that is *E. coli* O157:H7 and *S.* Typhimurium. These findings were considered to originate from the antibody–antigen reactions as well as the saturation of the unoccupied sites with BSA. The specific interaction between variable regions on the heavy chains and light chains of the antibody and the epitopes on the antigen

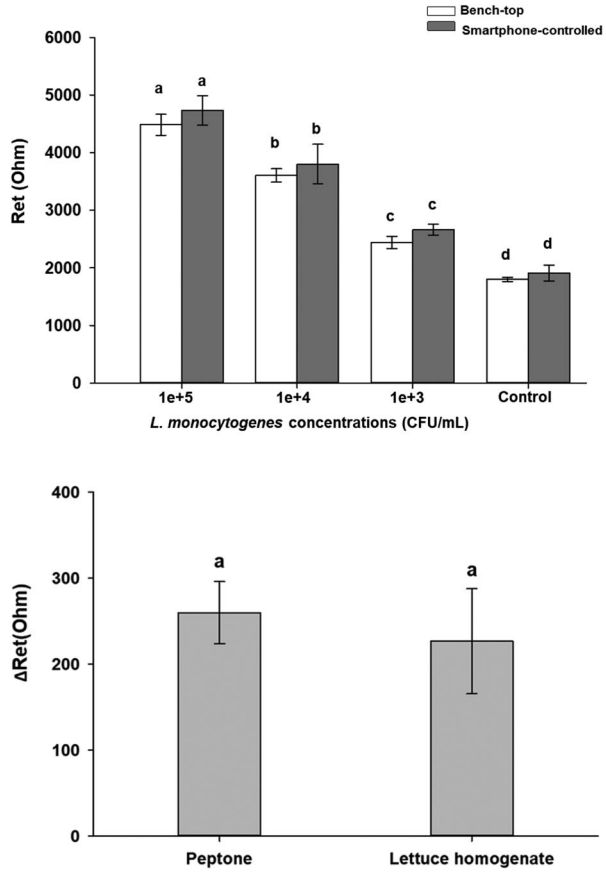


**FIGURE 4** Electron transfer resistance obtained by the bench-top and smartphone-controlled system in response to $10^3$–$10^5$ CFU/ml of L. monocytogenes (a) and the ΔRet of the sensor tested in lettuce homogenate

ensure the specificity of the sensor analysis (Killard et al., 1995). In addition, BSA serves as a blocking agent for its capability of saturating the unoccupied sites without participating in the immunochemical reactions in the assay (Jeyachandran et al., 2009).

## 3.3 | Performance of the smartphone-controlled platform for *L. monocytogenes* detection

The applicability of the proposed smartphone-controlled system was demonstrated by analyzing $R_{et}$ of the functionalized sensors and immunologically interacted sensors with comparison to the reference laboratory instrument. As shown in Figure 4a, the portable platform was able to detect the same range of concentrations of the target ($10^3$–$10^5$ CFU/ml) as the reference instrument. The control represents the $R_{et}$ of the sensors with coatings and thus, may have resulted in small variation. In addition, although slight variations were apparent, the obtained $R_{et}$ values were statistically comparable with the reference device. The slight variations in the values between the two systems could be partially attributed to the nonlinear nature of redox processes and discontinuities signal sampling at several characteristic frequencies (Jenkins et al., 2019).

A similar trend was observed in the study of Jenkins et al. (2019), in which the electrochemical impedance spectroscopy scanning of the bare and coated 50 μm gold-plated tungsten wires with both ABE-Stat and the reference laboratory device resulted in reasonably close data; however, slight deviations were present. Although unable to fully explain this phenomenon, the network analyzer chip used in the ABE-Stat may have resulted in variations and distortions at a certain frequency range when conducting the analyses (Jenkins et al., 2019). Despite the discrepancies, the presented platform significantly reduced the overall size and the cost of the platform compared to the reference laboratory potentiostat. The total cost of the ABE-Stat ranges from US$152.50 to US$215 depending on the quantity manufactured (Jenkins et al., 2019). This price is approximately 1% of the reference laboratory instrument. In terms of weight, the ABE-Stat potentiostat weighed only 2.7% of the reference laboratory device (4.99 kg).

## 3.4 | Detection of *L. monocytogenes* in lettuce homogenate

The accuracy of the proposed smartphone-controlled platform for the detection of *L. monocytogenes* in food samples was assessed by the recovery experiments. Prior to detecting the target bacterial cell, the influence of lettuce homogenate on the sensing signal was evaluated. The sensor was exposed to both target-free lettuce homogenate and sterilized peptone water (reference blank solution) and the $\Delta R_{et}$ values were compared. The results showed that the anti-*L. monocytogenes* sensor's responses to lettuce homogenate were not significantly different from the blank buffer solution (Figure 4b). This implies that lettuce homogenate did not alter the sensing signal of the sensor.

On the basis of the previous findings, lettuce homogenate was spiked with $10^3$–$10^5$ CFU/ml of *L. monocytogenes* and the $\Delta R_{et}$ was evaluated with both the reference device and smartphone-controlled platform. The recovery rates of the bacteria from lettuce homogenate were estimated as a ratio of model predictions ($\Delta R_{et}$ vs. CFU/ml) over the spiked concentrations. As shown in Table 2, the recovery percentage ranged from 88.48% to 95.38% for the bench-top and 90.21% to 93.69% for the proposed portable device. These high recovery rates indicate that the proposed platform was applicable for the detection of *L. monocytogenes* in real food systems.

**TABLE 2** Recoveries of *L. monocytogenes* in lettuce homogenate using the proposed method

| Sample | Original value (CFU/ml) | Spiked concentration (CFU/ml) | Detected (CFU/ml) | | Recovery (%) | |
|---|---|---|---|---|---|---|
| | | | Bench-top | Smartphone | Bench-top | Smartphone |
| 1 | 0 | $1.29 \times 10^3$ | $1.14 \times 10^3$ | $1.16 \times 10^3$ | 88.48 | 90.21 |
| 2 | 0 | $1.04 \times 10^4$ | $9.92 \times 10^3$ | $9.41 \times 10^3$ | 95.38 | 90.44 |
| 3 | 0 | $1.15 \times 10^5$ | $1.05 \times 10^5$ | $1.08 \times 10^5$ | 91.05 | 93.69 |

## 4 | CONCLUSION

In this study, a SWCNT-based electrochemical immunosensor for on-site detection of *L. monocytogenes* was developed. The limit of detection of the sensor was $10^3$ CFU/ml and an average detection time was 10 min. In addition, the sensor demonstrated high specificity and selectivity towards the target. In order to facilitate the requirements for on-site screening for food safety, the sensor was integrated into a smartphone-controlled platform. The performance of the proposed system was comparable to the reference instrument and exhibited high applicability for analyzing food samples.

Because the overall goal of this technology is to use as an on-site foodborne pathogen testing, the sensitivity of the sensor must be studied further. The current fabricated biosensor does not meet the industrial food safety requirement as the policy on *L. monocytogenes* in ready-to-eat foods is a zero (Archer, 2018; Shank et al., 1996). The sensitivity of the sensor could be enhanced by applying dielectrophoresis (DEP) force. DEP is the movement of particles in a solution that has been subjected to a nonuniform electric field (Pethig, 1996). DEP force can be used to electrically manipulate biological analytes within a fluid medium and increase the sensitivity. The sensing parameters such as the electrical conductivity, applied DEP voltage and frequency, and treatment time in detecting bacterial pathogens in food samples should be further investigated. In addition, superparamagnetic particles such as magnetic beads and magnetic nanoparticles could be utilized. The superparamagntic particles have been conjugated with various bioreceptors including antibodies and have shown to improve both the transduction signal and sensitivities due to their unique physical and chemical properties (Reverté et al., 2016; Wang et al., 2017). When subjected to an external magnetic field, the superparamagnetic particles are magnetized and enables the magnetic manipulation and thus, detection of the bacterial cells without affecting the biological interactions. The performance of the immunosensor depends highly on the performance of the antibody. The antibody–antigen interaction is influenced by several factors such as ionic strength, temperature, pH, concentrations of antigen and antibody, and cell viability (live/dead cells). Therefore, further studies should address the influence of the listed factors on the immobilization of antibodies as well as the affinity of the antibodies.

## ACKNOWLEDGMENTS

This project was supported by the USDA-Agricultural Research Service (Project No. 58-2040-8-010).

## AUTHORS CONTRIBUTIONS

**Bog Eum Lee**: Conceptualization; Investigation; Methodology; Writing original draft. **Taiyoung Kang**: Formal analysis; Writing review & editing. **Daniel Jenkins**: Formal analysis; Writing review & editing. **Yong Li**: Methodology; Validation. **Marisa M. Wall**: Funding acquisition. **Soojin Jun**: Conceptualization; Supervision; Writing review & editing

## CONFLICTS OF INTEREST

The authors have declared that there is no conflicts of interest.

## ORCID

*Soojin Jun* https://orcid.org/0000-0002-0865-4565

## REFERENCES

Allen, B. L., Kichambare, P. D., & Star, A. (2007). Carbon nanotube field-effect-transistor-based biosensors. *Advanced Materials*, *19*(11), 1439–1451.

Archer, D. L. (2018). The evolution of FDA's policy on Listeria monocytogenes in ready-to-eat foods in the United States. *Current Opinion in Food Science*, *20*, 64–68.

Arora, P., Sindhu, A., Dilbaghi, N., & Chaudhury, A. (2011). Biosensors as innovative tools for the detection of food borne pathogens. *Biosensors and Bioelectronics*, *28*(1), 1–12.

Bogomolova, A., Komarova, E., Reber, K., Gerasimov, T., Yavuz, O., Bhatt, S., & Aldissi, M. (2009). Challenges of electrochemical impedance spectroscopy in protein biosensing. *Analytical Chemistry*, *81*(10), 3944–3949.

Bourigua, S., Hnaien, M., Bessueille, F., Lagarde, F., Dzyadevych, S., Maaref, A., Bausells, J., Errachid, A., & Renault, N. J. (2010). Impedimetric immunosensor based on SWCNT-COOH modified gold microelectrodes for label-free detection of deep venous thrombosis biomarker. *Biosensors and Bioelectronics*, *26*(4), 1278–1282.

CDC. (2018). CDC and Food Safety. Retrieved from https://www.cdc.gov/foodsafety/cdc-and-food-safety.html

Chen, J., Zheng, X., Miao, F., Zhang, J., Cui, X., & Zheng, W. (2012). Engineering graphene/carbon nanotube hybrid for direct electron transfer of glucose oxidase and glucose biosensor. *Journal of Applied Electrochemistry*, *42*(10), 875–881.

Chen, Q., Wang, D., Cai, G., Xiong, Y., Li, Y., Wang, M., Huo, H., & Lin, J. (2016). Fast and sensitive detection of foodborne pathogen using electrochemical impedance analysis, urease catalysis and microfluidics. *Biosensors and Bioelectronics*, *86*, 770–776.

Chowdhury, A. D., De, A., Chaudhuri, C. R., Bandyopadhyay, K., & Sen, P. (2012). Label free polyaniline based impedimetric biosensor for detection of E. coli O157: H7 Bacteria. *Sensors and Actuators B: Chemical*, *171*, 916–923.

Darst, S. A., Ahlers, M., Meller, P. H., Kubalek, E. W., Blankenburg, R., Ribi, H. O., Ringsdorf, H., & Kornberg, R. D. (1991). Two-dimensional crystals of streptavidin on biotinylated lipid layers and their interactions with biotinylated macromolecules. *Biophysical Journal*, *59*(2), 387–396.

Ferrier, D. C., Shaver, M. P., & Hands, P. J. W. (2015). Micro-and nanostructure based oligonucleotide sensors. *Biosensors and Bioelectronics*, *68*, 798–810.

Heller, I., Janssens, A. M., Männik, J., Minot, E. D., Lemay, S. G., & Dekker, C. (2008). Identifying the mechanism of biosensing with carbon nanotube transistors. *Nano Letters*, *8*(2), 591–595.

Jadhav, S., Bhave, M., & Palombo, E. A. (2012). Methods used for the detection and subtyping of *Listeria monocytogenes*. *Journal of Microbiological Methods*, *88*(3), 327–341.

Jain, S., Singh, S. R., Horn, D. W., Davis, V. A., Ram, M. J., & Pillai, S. R. (2012). Development of an antibody functionalized carbon nanotube biosensor for foodborne bacterial pathogens. *J Biosens Bioelectron*, *11*, 2.

Jenkins, D. M., Lee, B. E., Jun, S., Reyes-De-Corcuera, J., & McLamore, E. S. (2019). ABE-Stat, a fully open-source and versatile wireless potentiostat project including electrochemical impedance spectroscopy. *Journal of The Electrochemical Society*, *166*(9), B3056–B3065.

Jeyachandran, Y. L., Mielczarski, E., Rai, B., & Mielczarski, J. A. (2009). Quantitative and qualitative evaluation of adsorption/desorption of bovine serum albumin on hydrophilic and hydrophobic surfaces. *Langmuir*, *25*(19), 11614–11620.

Killard, A. J., Deasy, B., O'Kennedy, R., & Smyth, M. R. (1995). Antibodies: Production, functions and applications in biosensors. *TrAC Trends in Analytical Chemistry*, *14*(6), 257–266.

Liu, Y.-X., Yuan, D.-X., Yan, J.-M., Li, Q.-L., & Ouyang, T. (2011). Electrochemical removal of chromium from aqueous solutions using electrodes of stainless steel nets coated with single wall carbon nanotubes. *Journal of Hazardous Materials*, *186*(1), 473–480.

Lu, L., Chee, G., Yamada, K., & Jun, S. (2013). Electrochemical impedance spectroscopic technique with a functionalized microwire sensor for rapid detection of foodbornepathogens. *Biosensors and Bioelectronics*, *42*, 492–495.

Majumdar, T., Chakraborty, R., & Raychaudhuri, U. (2013). Development of PEI-GA modified antibody based sensor for the detection of *S. aureus* in food samples. *Food Bioscience*, *4*, 38–45.

Mao, Y., Huang, X., Xiong, S., Xu, H., Aguilar, Z. P., & Xiong, Y. (2016). Large-volume immunomagnetic separation combined with multiplex PCR assay for simultaneous detection of *Listeria monocytogenes* and *Listeria ivanovii* in lettuce. *Food Control*, *59*, 601–608.

Mello, L. D., & Kubota, L. T. (2002). Review of the use of biosensors as analytical tools in the food and drink industries. *Food Chemistry*, *77*(2), 237–256.

Pethig, R. (1996). Dielectrophoresis: Using inhomogeneous AC electrical fields to separate and manipulate cells. *Critical Reviews in Biotechnology*, *16*(4), 331–348.

Prodromidis, M. I. (2010). Impedimetric immunosensors—A review. *Electrochimica Acta*, *55*(14), 4227–4233.

Reverté, L., Prieto-Simón, B., & Campàs, M. (2016). New advances in electrochemical biosensors for the detection of toxins: Nanomaterials, magnetic beads and microfluidics systems. A review. *Analytica Chimica Acta*, *908*, 8–21.

Rodriguez, B. A., Trindade, E. K., Cabral, D. G., Soares, E. C., Menezes, C. E., Ferreira, D. C., & Dutra, R. F. (2015). Nanomaterials for advancing the health immunosensor. *Biosensors-Micro and Nanoscale Applications*, 347–374.

Rouse, J. H., Lillehei, P. T., Sanderson, J., & Siochi, E. J. (2004). Polymer/single-walled carbon nanotube films assembled via donor–acceptor interactions and their use as scaffolds for silica deposition. *Chemistry of Materials*, *16*(20), 3904–3910.

Shank, F. R., Elliot, E. L., Wachsmuth, I. K., & Losikoff, M. E. (1996). US position on *Listeria monocytogenes* in foods. *Food Control*, *7*(4–5), 229–234.

Sharma, H., & Mutharasan, R. (2013). Review of biosensors for foodborne pathogens and toxins. *Sensors and Actuators B: Chemical*, *183*, 535–549.

Wang, T., Zhou, Y., Lei, C., Luo, J., Xie, S., & Pu, H. (2017). Magnetic impedance biosensor: A review. *Biosensors and Bioelectronics*, *90*, 418–435.

Wang, Y., Ye, Z., & Ying, Y. (2012). New trends in impedimetric biosensors for the detection of foodborne pathogenic bacteria. *Sensors*, *12*(3), 3449–3471.

Yamada, K., Kim, C.-T., Kim, J.-H., Chung, J.-H., Lee, H. G., & Jun, S. (2014). Single walled carbon nanotube-based junction biosensor for detection of *Escherichia coli*. *Plos One*, *9*(9), e105767.

Yang, L., & Bashir, R. (2008). Electrical/electrochemical impedance for rapid detection of foodborne pathogenic bacteria. *Biotechnology advances*, *26*(2), 135–150.

Zhu, Q., Gooneratne, R., & Hussain, M. (2017). Listeria monocytogenes in fresh produce: Outbreaks, prevalence and contamination levels. *Foods*, *6*(3), 21.

**How to cite this article:** Lee, B. E., Kang, T., Jenkins, D., Li, Y., Wall, M. M., & Jun, S. (2022). A single-walled carbon nanotubes-based electrochemical impedance immunosensor for on-site detection of *Listeria monocytogenes*. *Journal of Food Science*. *87,* 280–288. https://doi.org/10.1111/1750-3841.15996